A Molecular Dynamics Study of Epoxy-Based Networks: Cross-Linking Procedure and Prediction of Molecular and Material Properties

Vikas Varshney,*,†,‡ Soumya S. Patnaik,‡ Ajit K. Roy,‡ and Barry L. Farmer‡

Universal Technology Corporation, Dayton, Ohio 45432 and Materials and Manufacturing Directorate, Air Force Research Laboratory, Wright Patterson AFB, Dayton, Ohio 45433-7750

Received May 23, 2008; Revised Manuscript Received July 9, 2008

ABSTRACT: Molecular modeling of thermosetting polymers has been presented with special emphasis on building atomistic models. Different approaches to build highly cross-linked polymer networks are discussed. A multistep relaxation procedure for relaxing the molecular topology during cross-linking is proposed. This methodology is then applied to an epoxy-based thermoset (EPON-862/DETDA). Several materials properties such as density, glass transition temperature, thermal expansion coefficient, and volume shrinkage during curing are calculated and found to be in good agreement with experimental results. Along with the material's properties, the simulations also highlight the distribution of molecular weight buildup and inception of gel point during the network formation.

Introduction

With the advancement and sophistication in various experimental and characterization techniques[1] over the past decade, "nanotechnology" has emerged as a revolutionizing field aimed at understanding different physical and chemical phenomena at the molecular level and thereby facilitating the development of micro- and nanoscale devices with desired properties. At these length scales, along with other properties, high structural integrity is often desired in order to provide better stability for such devices. Epoxy-based networks are one such class of materials which possess excellent mechanical properties for structural stability.[2] Indeed, these materials are often used in aerospace as well as electronic industry as adhesives, coatings, and composites. In addition, a lot of interest has also developed in recent years to study thermal and electrical conductivity of these composites with nanofillers (such as carbon nanotubes) to explore the possibility of building structurally stable micro- and nanoscale composites devices.

Computer simulations provide an excellent route to study these networks. While on one hand, they can reduce trial and error experimentation; on the other hand, they provide insightful information at molecular as well as micro length scales which are often not extracted from experiments. Molecular dynamics (MD) simulations[3] which consider atomic details have been very successful in exploring various phenomena occurring at pico- to nanosecond time scales and relating these phenomena to the structure and molecular chemistry. MD simulations also possess an inherent advantage over continuum modeling in addressing nanoscale interfacial issues which are significant for nanocomposites.

Along with a realistic force field, MD simulations also require a molecular model. The formation of computer models for cross-linked network has been studied by several authors. The early motivations back in the 1980s and 1990s mainly focused on understanding the reaction kinetics of cross-linking process using lattice[4] as well as nonlattice[5] Monte Carlo simulations in terms of degree of polymerization, molecular weight distribution, polydispersity, sol−gel transition, etc.[6] Most of these studies were primarily mathematical in nature, which did not take into account the topological information on the network. So, useful information related to mechanical as well as thermodynamic properties was lost. Later on, several authors studied the formation of cross-linked network with topological information through several cross-linking approaches using molecular dynamics simulations. Specifically, Doherty[7] and co-workers created PMA networks using lattice-based simulations using polymerization molecular dynamics scheme. Yarovsky et al.[8] have presented a methodology to cross-link low molecular weight water-soluble phosphate-modified epoxy resins (CYMEL 1158). However, all the cross-linking reactions was carried out simultaneously (in a single step) in a three-step procedure in their study.

Recently, Gou et al.[9] built cross-linked network for epoxy resins (EPON-862) using Accelyrs[10] to study interfacial interactions between CNTs and cured epoxy resin in terms of stress transfer. Similarly, Fan et al.[11] evaluated material properties of EPON-862 cured with TETA curing agent using the Accelyrs Simulation package. Although both studies provided insightful information regarding material properties and interfacial interactions, no details were provided regarding the cross-linking procedure. Xu et al.[12] have also performed cross-linking simulations for epoxy resin and used their model to study diffusion of water in these cross-linked networks.[13] The authors used an iterative MD/MM procedure to cross-link epoxy resin (DGEBA) where the newly formed topology is subjected to 1000 MD steps of relaxation. This approach carries out one cross-link per iteration, which is bound to have computational limitations when applied to cross-linking of larger systems.

It should be noted that most simulation studies on formation of cross-linked network discussed so far have been done for quite small model systems. Heine et al.[14] simulated structural and mechanical properties of large PDMS networks, modeled as united atom model, using a dynamic cross-linking approach based on cutoff distance criterion. Here, the newly formed topology was relaxed using a modified potential which was linear at large distances and quadratic at short distances. Recently, Liao et al. have also studied formation of polymer networks on a coarse-grain level based on varying ratios of cross-linkers to polymer chain ends.[15] It is worth noting that although the degree of cross-linking is known to govern the bulk effective properties in many cases, simulations that capture these properties as a function of cross-linking have not been carried out until very recently where Komarov et al. used a four-

* Corresponding author: E-mail: vikas.varshney@afmcx.net.
† Universal Technology Corporation.
‡ Air Force Research Laboratory.

10.1021/ma801153e CCC: $40.75
Published on Web 08/21/2008

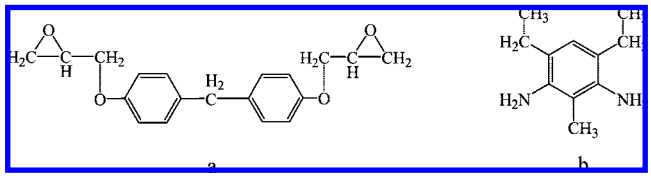

Figure 1. Molecular structure of (a) EPON-862 and (b) DETDA.

step reverse mapping procedure using the MC/MD hybrid scheme to study the physical behavior of highly dense network as a function of cure conversion.[16]

In the sprit of the above discussion and to provide a more robust approach to model network polymers, we provide a stepwise procedure to build a highly cross-linked system of epoxy-based networks (EPON-862 and DETDA as a model system) which can be generalized to other cross-linked systems as well. To achieve cross-linking network of relatively larger system of epoxy resins, we have coupled Heine's dynamic cross-linking concept[14] at the atomistic level with Xu's iterative MD/MM concept.[12] Additionally, we propose a new multistep topology relaxation procedure formed during new bond formation. We also investigate cross-linking based on different criteria and study them in terms of inter- and intramolecular energies and computational times as a function of cross-linking. The present article therefore covers a broader perspective of the cross-linked networks, including characterization of various thermodynamic as well as structural properties as a function of temperature and degree of curing.

The article is organized as follows. In the next section, we present our simulation strategy with the main focus on cross-linking procedure. Thereafter, we present our results on analysis of thermodynamic and molecular properties as a function of cross-linking. We also compare our results with other available experimental and simulation studies.

Simulation Details

The initial model system consists of un-cross-linked epoxy resin EPON-862 (diglycidyl ether of bisphenol F) and cross-linking agent EPI-Cure-W (diethylenetoluenediamine, DETDA). The model system is shown in Figure 1. The molecular models were built using the model building tools of Insight II.[10] A stoichiometric mixture of 16 EPON-862 molecules and 8 DETDA molecules was built using the amorphous cell module with charges assigned using the group charge method. For future reference, we will refer this as the (16, 8) system where the first and second indices stand for number of epoxy resin and cross-linking agent molecules, respectively. All the simulations were performed using CVFF (consistent valence force field)[10,17] using LAMMPS molecular dynamics software[18] as provided by Sandia National Laboratories. The nonbonded van der Waals interactions were modeled as the 12−6 LJ potential. In addition, the PPPM (particle−particle−particle mesh) technique[19] was used to include long-range Columbic interactions. The initial system was equilibrated using NVT and NPT simulations at 300 K and atmospheric pressure for 100 ps. The Nose-Hoover thermostat and barostat were used for temperature and pressure control respectively. 3-D periodic boundary conditions were employed for all simulations to remove possible surface effects. Once the system was equilibrated, the cross-linking was performed as discussed below.

The cross-linking procedure was divided into three main steps, namely, activation, cross-linking, and saturation.

Activation. In this step, all potential reactive sites are activated for both epoxy resin and curing agent as discussed by Xu.[12] This is done by first hydrating epoxy oxygen atoms at the ends and creating a reactive methylene end group by removing one of its hydrogen atoms. In case of curing agent, DETDA, both hydrogen atoms are removed from DETDA's amine group to make it chemically active. In addition, the partial charges are also adjusted on these potentially reactive carbon and nitrogen atoms in respective molecules to retain the neutrality of the whole system. The activation step is shown schematically in Figure 2.

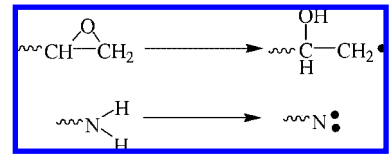

Figure 2. Activation of epoxy and amine ends for the cross-linking reaction. The symbol (●) attached to C and N shows their activity toward the cross-linking reaction.

Cross-Linking Approaches. *Approach 1*: Assumes equal reactivity of primary and secondary amine.

Approach 2: Assumes that primary amine has much higher reactivity than secondary amine. In this case, all the nitrogen atoms are reacted once before any secondary reaction starts.

Approach 3: A nitrogen atom is selected randomly and is fully reacted (twice) before another nitrogen atom starts reacting. This approach was employed to study dihedral energy buildup during the course of the cross-linking as discussed later.

Approach 4: A dynamic cross-linking approach: all potential reactive pairs are reacted simultaneously within the cutoff in compliance with the equal reactivity assumption. The motivation for studying approaches 2 and 3 in addition to approaches 1 (used by Xu[12]) and 4 (used by Heine[14]) was to explore their effect if any, in achieving better equilibrated cross-linked structures with lower energies.

Algorithm. A flowchart describing the cross-linking algorithm is shown in Figure 3 and is discussed below.

Step 1: Initial cutoff distances as well as cross-linking limits (in terms of %) are defined for the cross-linking algorithm. For approaches 1−3, single upper bound cutoff distances (10 Å) and, for approach 4, a lower bound cutoff distance (4 Å) are defined. Although initially, the cross-linking limit is set to be 100%, it is allowed to be stopped at any time.

Step 2: In this step, the system is equilibrated using NPT simulations for 40 ps. Since it is important to ascertain that the simulation time in between successive reactions is sufficiently long for the unreacted reactive species to move around, it was chosen on the basis of the calculated root-mean-square distance (rmsd). The rmsd of reactive carbon and nitrogen atoms was found to be ∼4.6 and ∼4.2 Å in 40 ps, respectively, thus ensuring that our equilibration time is reasonably long to provide a good mixing of the various species. Although the diffusion of the cross-linking entities decays as cross-linking progresses, the aforementioned values of rmsd of reactive carbon and nitrogen atoms should provide a preliminary approach toward system relaxation prior to next cross-linking.

Step 3: In this step, all potential un-cross-linked reactive pairs are identified. In addition, all pairs that could lead to possible catenation in the network are removed from this list. For approaches 1−3, the minimum distance pair is then selected, and a bond is formed if this distance is less than the upper bound cutoff. On the other hand, for case 4, all bonds within the lower bound cutoff distance are created.

Step 4a: If cross-linking does occur, the topological information is updated by introducing new bonds, angles, dihedral angles, and improper angles into the system. Thereafter, the topology is relaxed using a multistep relaxation procedure, which essentially resists abrupt change in the spatial coordinates of atoms in the vicinity of the newly formed bond and ensures a

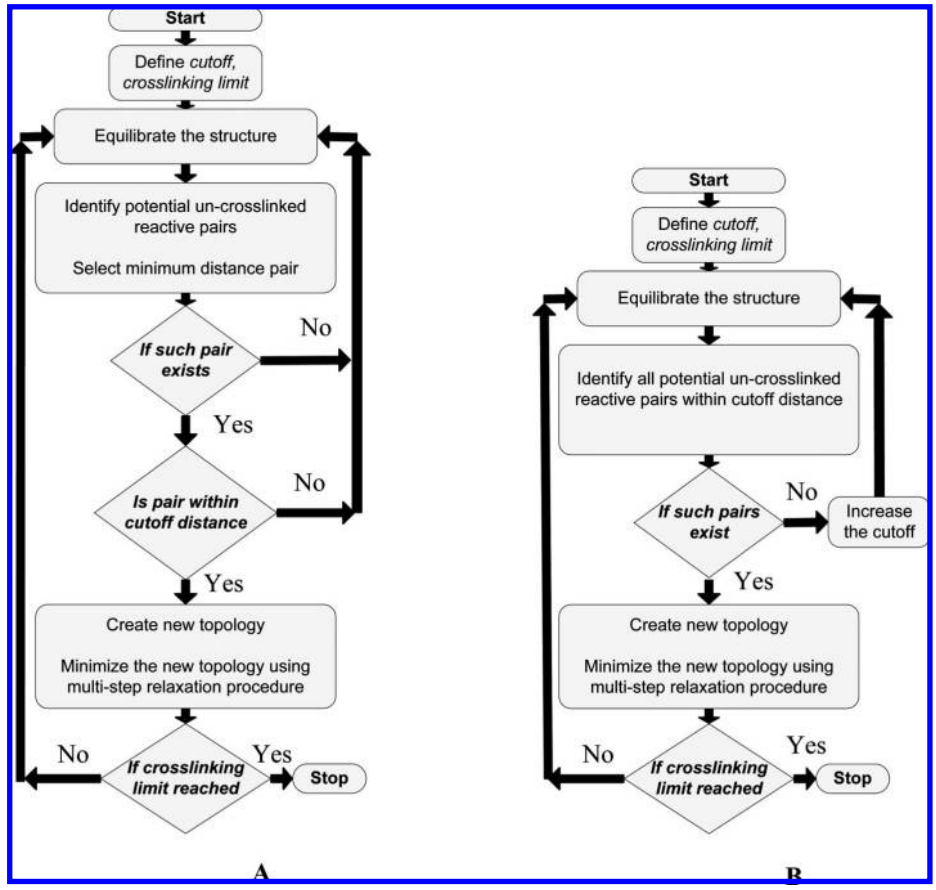

Figure 3. Cross-linking algorithm: (A) approaches 1−3 and (B) approach 4.

Table 1. Multistep Relaxation Procedure

steps	effective force constant[a]	effective equilibrium bond length[b]
step 1	$k_0/5$	$r_0 + 4 \times (r - r_0)/5$
step 2	$2 \times k_0/5$	$r_0 + 3 \times (r - r_0)/5$
step 3	$3 \times k_0/5$	$r_0 + 2 \times (r - r_0)/5$
step 4	$4 \times k_0/5$	$r_0 + 1 \times (r - r_0)/5$
step 5	k_0	r_0

[a] k_0 defines equilibrium force constant. [b] r_0 defines equilibrium bond length; r is the initial cross-linking distance.

slow relaxation of atoms in the newly formed topology. In this procedure, the force constant of the new bond is gradually increased from zero to its equilibrium value, and the equilibrium bond length is decreased from its original distance to its actual equilibrium value, in a series of steps (five, for our approach as shown in Table 1). The system is minimized at each step with these effective bond parameters.

Step 4b: If cross-linking does not occur, the system is further equilibrated according to step 2. However, for approach 4, the lower bound cutoff distance is increased by 0.25 Å in the subsequent iteration.

Step 5: After the minimization, if cross-linking limit is not reached, the algorithm jumps to step 2 where the equilibration of the new structure is performed; else the simulations are stopped.

Saturation. Once the cross-linking is complete, the remaining active sites on unreacted amine nitrogen atoms and epoxy carbon atoms are saturated with hydrogen atoms. The partial atomic charges on these complementary atoms are also adjusted to keep the system neutral. It is worth noting that once a cross-link is created between amine nitrogen and epoxy carbon, the charge distribution around these atoms is going to change. In order to take this into account, charges were evaluated on a model molecule using Insight II,[10] as shown in Figure 4 which has a

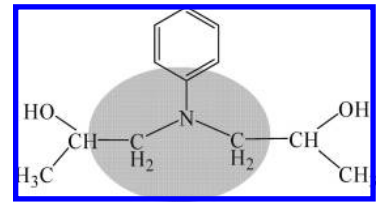

Figure 4. Shaded section of the molecule represents the cross-linking surroundings in which charges were redistributed.

molecular topology similar to the newly formed cross-link. Then, the original charge distribution around the new cross-links was replaced by charge distribution shown in the shaded region of Figure 4, keeping the system neutral. The details of the charge distribution are provided as Supporting Information.

In order to achieve a relaxed network, the cross-linked system is further equilibrated at zero pressure using constant pressure simulations by first heating at 600 K for 100 ps followed by annealing to 300 K in 6 ns.

Although the above methodology has been discussed for the (16, 8) system size, we also performed cross-linking simulations for relatively larger (128, 64) and (256, 128) systems using the dynamic cross-linking approach as discussed above. One of such cross-linked system along with the cross-linking entities is shown in Figure 5. The use of this dynamic cross-linking approach over other approaches should become more transparent during the discussion concerning comparisons of different approaches used to cross-link (16, 8) systems as presented in the next section.

Results and Discussion

This section is broadly divided into two subsections. The first part briefly deals with comparison of various cross-linking

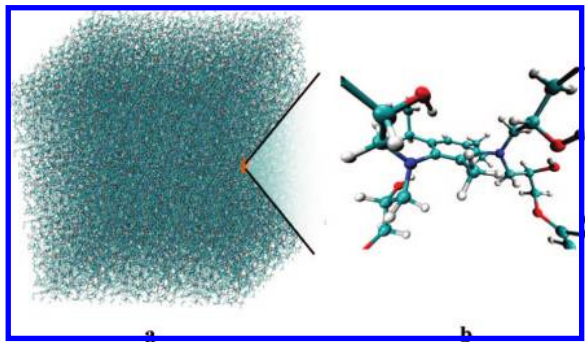

Figure 5. (a) Formation of the cross-linked network as discussed in text. (b) Depiction of cross-link as formed in the system through a zoomed-in version of the network. Color code: carbon (cyan); oxygen (red); nitrogen (blue); and hydrogen (white).

approaches, discussed for smaller (16, 8) systems. The second part focuses on the evaluation of various material properties for bigger (128, 64) cross-linked systems.

The intra- and intermolecular energies are listed in Table 2 for un-cross-linked and cross-linked systems using different approaches. Some of the important points to note are as follows:

(a) All energies except Coulombic energy increase on cross-linking. Xu et al.[12] have also reported such increase in energetic components upon cross-linking based on Dreiding force field.

(b) The rise in bond, angle, and dihedral energies can be attributed to the newly formed topology.

(c) The dynamic cross-linking approach (approach 4) leads to a better equilibrated structure (as seen by the lowest values of the energetic components).

(d) The dynamic cross-linking approach also has another advantage with its relatively shorter computational time. In further support of dynamic cross-linking approach, we would like to point out that for cross-linking of larger (128, 64) system with 256 possible cross-links ~95% cross-linking was achieved in only 75 iterations. This shows a significant reduction (one-third) in computational time for cross-linking with respect to the other three approaches which would take more than 250 iterations on the whole for same amount of cross-linking.

The observation of the proximity of reactive sites during the cross-linking stage using various approaches is worth mentioning. Figure 6 shows the initial distance at which bond is formed as curing progresses with dynamic cross-linking procedure for the (128, 64) cube system. As seen from the figure, about 80−90% of the cross-linking has been successfully achieved within the cutoff distance of 4 and 5.5 Å, respectively. The figure clearly shows that using the dynamic cross-linking approach as discussed before, a well-relaxed cross-linked network can be attained successfully without imposing any cross-linking strain within significantly less iterations as compared to other approaches. In the remaining part of this section, various material properties will be analyzed for the (128, 64) system.

For epoxy-based systems, volume shrinkage or increase in density is observed experimentally during the process of network formation.[2] In order to observe this shrinkage, the instantaneous volume of the system during the relaxation stage of cross-linking simulations was tracked continuously. The resulting equilibrated volume as curing progresses is shown in Figure 7. For highly dense system (~90% cross-linking), a volume shrinkage of 7% was observed in our simulations. Given the complexity of the cross-linking process, the results provide a good estimation of volume shrinkage with respect to cross-linking process. The results are also in accordance with an increase in density with cure conversion as reported recently by Kamorov[16] and volume shrinkage results as observed by Yarovski[8] where the authors observe a volume shrinkage of 5−12% for different studied systems. It is also important to note here that such a volume shrinkage was not convincingly observed in case of the smaller (16, 8) systems due to significant statistical variations as shown in inset of Figure 7. Such an observation provides additional motivation to perform, study, and analyze simulations on larger systems.

To study the temperature dependence of various thermodynamic quantities, an annealing simulation was performed where the cross-linked system was slowly cooled down at the rate of 10 K/200 ps from 500 to 200 K under atmospheric pressure which was controlled by a Nose-Hoover thermostat and barostat. The change of density as a function of temperature is plotted in Figure 8. The density at room temperature was found to be 1.12 g/cm^3, which is in good agreement with experiments.[20] A kink in the density vs temperature slope is observed in Figure 8. The kink is usually identified as the glass transition temperature (T_g), which in our case occurs around 105 °C. The T_g is a second-order transition, and its value is often governed by cooling rate as well as method of measurement. The predicted T_g from our simulations are in fair agreement with experimental[20] as well as simulation results[11] on similar systems.

Coefficient of thermal expansion is another thermodynamic property which is of great importance in composite materials as they are used at various temperatures in practical applications. The coefficient of volume thermal expansion (CVTE), α, is defined as

$$\alpha = \frac{1}{V}\left(\frac{\partial V}{\partial T}\right)_P \tag{1}$$

where V, T, and P are the volume, temperature, and pressure of the system, respectively. For isotropic materials, the coefficient of linear thermal expansion (CLTE), β, is related to α as

$$\beta = \alpha/3 \tag{2}$$

The fractional change in volume (dV/V) vs temperature is plotted in Figure 9, and as expected, a kink suggestive of the T_g is observed around 105 °C. Additionally, the slope from the Figure 9 can also be identified as CVTE, α. Using eq 2, the calculated value of CLTE were found to be 40 ppm/°C around room temperature. The estimated value of CLTE is roughly two-thirds with respect to the experimental[21] findings (~62 ppm/°C) and other simulation studies[11] on similar epoxy systems and could be attributed to the differences in the experimental cooling rates and those employed in our simulation studies.

In addition to thermodynamic properties, it is also important to appreciate the kinetics of network formation which eventually determines its molecular structure. These processes are governed by reaction rates of the various reactions and analyzed by monitoring the molecular weight buildup and distribution, cycle ranks, and gel point formation using experimental techniques such as chromatography, etc. To provide further insight into the network formation, we show the buildup of weight-average molecular weight, M_w, as a function of cure conversion in Figure 10, based on dynamic cross-linking approach (approach 4). The figure shows that most of the rise in the molecular weight happens toward higher cure conversion (~0.65−0.75). This trend of molecular weight buildup is in accordance with the principle of step-growth polymerization, the same approach which is used to cure epoxy resins experimentally. The figure also shows the buildup of molecular weight of the largest group within the system, the inception of secondary cycles and their trend, and the theoretical gel point (0.577) as predicted by branching theory for bifunctional epoxy resins and tetrafunctional cross-linkers.[22] A secondary cycle is defined as an intramolecular reaction happening within a group. The inception of the secondary cycles has also been treated as a gel point in the literature.[22] From the figure, it is quite clear that in our simulations the inception of secondary cycles occurs around

Table 2. Comparison of Various Cross-Linking Approaches

quantities[a]	un-cross-linked system	cross-linked systems (30/32 cross-links)			
		approach 1	approach 2	approach 3	approach 4
bond energy (per unit)	419 (0.44)	471 (0.48)	473 (0.48)	472 (0.48)	468 (0.48)
angle energy (per unit)	99 (0.06)	165 (0.09)	172 (0.1)	168 (0.1)	164 (0.09)
dihedral energy (per unit)	129 (0.06)	440 (0.18)	441 (0.18)	418 (0.17)	423 (0.17)
van der Waals energy	580	774	758	774	754
Columbic energy	−349	−355	−335	−341	−350
total energy	231	419	423	433	404
computational time[b] (iterations)	N/A	32	32	31	23

[a] Energy units are in kcal/mol. Per unit quantities for respective energies are shown in parentheses. [b] The computational time is given in terms of number of iterations since every iteration has same equilibration time (per iteration) irrespective of the approach.

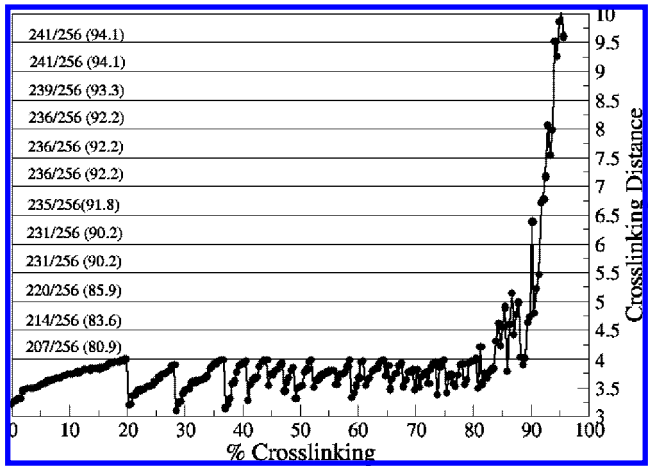

Figure 6. Plot of initial cross-linking (bond formation) distance (Å) as a function of cross-linking. The labels in the *Y* abscissa represent the number of current cross-links/number of possible cross-links (maximum % cross-linking attained at current cross-linking distance).

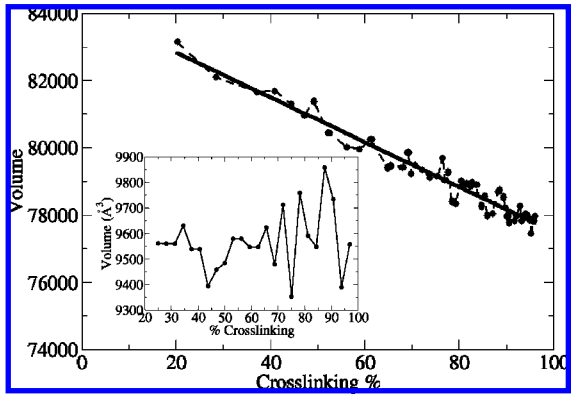

Figure 7. Plot of volume shrinkage as a function of cross-linking %. Inset shows a similar plot for the (16, 8) system with the dynamic cross-linking approach.

0.57, providing good agreement between simulation results and theoretical predictions. The gel point can also be estimated from the inflection point of the largest group molecular weight buildup. Although it is quite difficult to identify the inflection point with great accuracy from Figure 10, one can safely say that it seems to be occurring between 0.6 and 0.65, providing a good estimation of gel point. Here, we would also like to point that that toward higher cure conversion (>0.8) most of the reactions happening are intramolecular reactions. This is supported by the fact that in this region a linear increase in number of secondary cycles is observed as a function of cure conversion along with negligible buildup of molecular weight.

It is known from the literature that near the gel point the probability of reaction between largest and second largest group is maximum, giving rise to a sharp increase in molecular weight

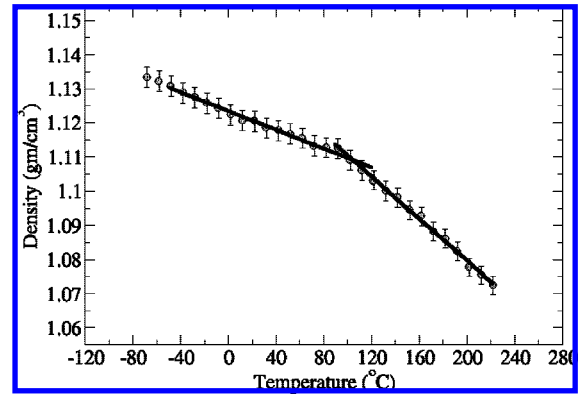

Figure 8. Plot of density variation as a function of temperature.

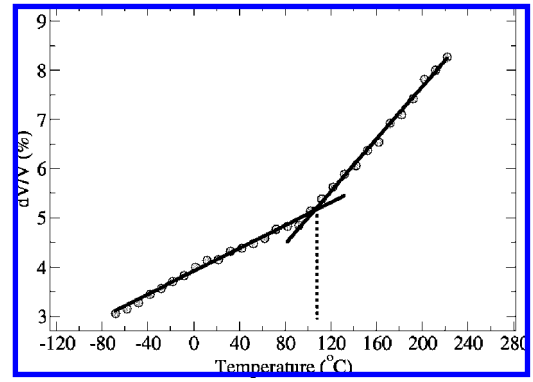

Figure 9. Plot of fractional volume change as a function of temperature. The dotted line shows the glass transition temperature (T_g).

of largest group at the inflection point. This also implies that, after this reaction, most of the subsequent reactions are going to occur within this largest group, thus corroborating with the concept of inception of secondary cycles. Chiu and co-workers[6] performed Monte Carlo simulations on curing of epoxides with amines and estimated the gel point using the weight-averaged reduced molecular weight (RMW) approach. RMW is defined as the weight-average molecular weight of all reacting groups except the largest one. One can easily foresee that the RMW first increases with cure conversion and then decreases. Here, the maximum in RMW is also characterized as a gel point. In order to compare our approach with that of Chiu et al., we have also estimated the gel point using the RMW approach. The results are presented in Figure 11 where molecular weights of largest group, second largest group, and weight-averaged reduced molecular weight are plotted as a function of cure conversion. It is clear from the figure that the maximum in second largest as well as RMW occurs within close proximity of the theoretical gel point which provided us with confidence in our cross-linking approach. Here, it is worth mentioning that both peaks in Figure 11 are quite broad due to limitations of system size (only 256 possible cross-links). However, we

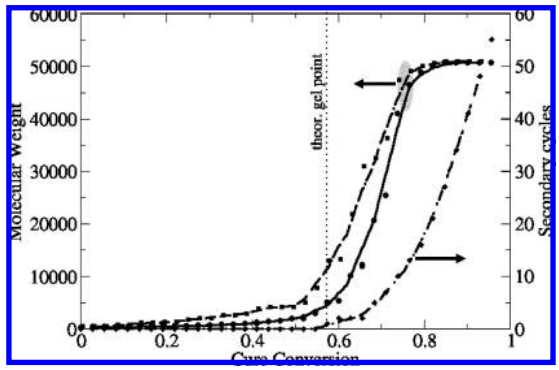

Figure 10. Plot of weight-average molecular weight (circles), largest molecular weight (squares), and secondary cycles (diamonds) as a function of cure conversion. The dashed lines are a guide to the eyes. The dotted line suggests the theoretical gel point.

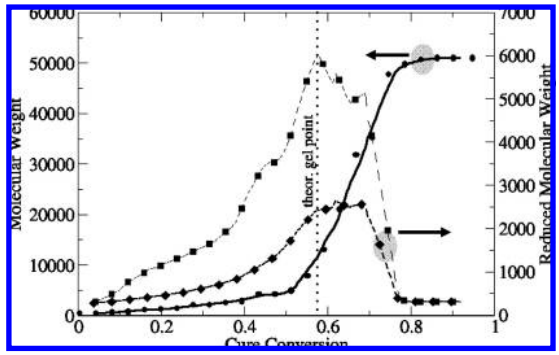

Figure 11. Plot of molecular weight of largest group (circles), second-largest group (squares), and weight-averaged reduced molecular weight (diamonds) as a function of cure conversion. The dashed lines are a guide to the eyes. The dotted line suggests the theoretical gel point.

postulate that the width of these peaks should decay as the size of the system increases.

Summary

The present article provides a detailed and clear discussion of an improved method of developing relaxed cross-linked networks. Our dynamic cross-linking approach is compared with other previously developed methods and found to be more efficient in building larger cross-linking networks as it significantly reduces the computational time and leads to better equilibrated structures with lower energies. Although the procedure is discussed for EPON-862/DETDA as a model epoxy systems, in principle, the same approach could be used to build other cross-linked networks. Simulations were carried out to investigate various thermodynamic and structural properties as a function of degree of curing, and the resulting values were found to be in good agreement with experimental results, a significant accomplishment demonstrating the promise of MD tools for molecular simulation of thermoset polymers. These network models are being currently used for studying thermal conductivity of nanocomposites.

Acknowledgment. This work was performed under U.S. Air Force Contract F33615-030D-5801, 0059. The lead two authors (Varshney and Patnaik) greatly appreciate partial funding from AFOSR in performing this work. The authors thank Dr. Tia Benson Tolle for pointing them to the problem and Dr. Taner Drama for his helpful discussions regarding the cross-linking procedure.

Supporting Information Available: Description of the charge update strategy after the cross-linking procedure. This material is available free of charge via the Internet at http://pubs.acs.org.

References and Notes

(1) Dupas, C.; Houdy; P.; Lahmani, M. *Nanoscience*; Springer: Berlin, 2007.
(2) May, C. A. *Epoxy Resins*; Dekker: New York, 1988.
(3) Frenkel, D.; Smit B. *Understanding Molecular Simulation: From Algorithms to Applications*; Elsevier: New York, 2002.
(4) (a) Schulz, M.; Frisch, H. L. *J. Chem. Phys.* **1994**, *101*, 10008. (b) Rohr, D. F.; Klein, M. T. *Ind. Eng. Chem. Res.* **1990**, *29*, 1210.
(5) Eichinger, B. E.; Shy, L. Y.; Leung, Y. K. *Macromolecules* **1985**, *18*, 983.
(6) (a) Chiu, W. Y.; Cheng, K. C. *Macromolecules* **1994**, *27*, 3406. (b) Chiu, W. Y.; Chen, Y. C. *Macromolecules* **2000**, *33*, 6672.
(7) Doherty, D. C.; Holmes, B. N.; Leung, P.; Ross, R. B. *Comput. Theor. Polym. Sci.* **1998**, *8*, 169.
(8) Yarovsky, I.; Evans, E. *Polymer* **2002**, *43*, 963.
(9) Gou, J. H.; Minaie, B.; Wang, B.; Liang, Z. Y.; Zhang, C. *Comput. Mater. Sci.* **2004**, *31*, 225.
(10) Accelrys Inc., San Diego, CA.
(11) Fan, H. B.; Yuen, M. M. F. *Polymer* **2007**, *48*, 2174.
(12) Wu, C. F.; Xu, W. J. *Polymer* **2006**, *47*, 6004.
(13) Wu, C. F.; Xu, W. J. *Polymer* **2007**, *48*, 5440.
(14) Heine, D. R.; Grest, G. S.; Lorenz, C. D.; Tsige, M.; Stevens, M. J. *Macromolecules* **2004**, *37*, 3857.
(15) Yang, W.; Wei, D.; Jin, X.; Liao, Q. *Macromol. Theory Simul.* **2007**, *16*, 548.
(16) Komarov, P. V.; Yu-Tsung, C.; Shih-Ming, C.; Khalatur, P. G.; Peineker, P. *Macromolecules* **2007**, *40*, 8104.
(17) Dauber-Osguthorpe, P.; Roberts, V. A.; Osguthorpe, D. J.; Wolff, J.; Genest, M.; Hagler, A. T. *Proteins: Struct., Funct., Genet.* **1988**, *4*, 31.
(18) Plimpton, S. J. *J. Comput. Phys.* **1995**, *117*, 1.
(19) Hockney, R. W.; Eastwood J. W. *Computer Simulation Using Particles*; Taylor & Francis Group: New York, 1988.
(20) Literature from resolution performance products, http://www.resins.com/resins/am/pdf/SC1183.pdf.
(21) Wang, S.; Liang, Z.; Gonnet, P.; Liao, Y.-H.; Wang, B.; Zhang, C. *Adv. Funct. Mater.* **2007**, *17*, 87.
(22) Hadicke, E.; Stutz, H. *J. Appl. Polym. Sci.* **2002**, *85*, 929.

MA801153E